Template Polymerization of *N*-Vinylimidazole along Poly(methacrylic acid) in Water. 4. Complex Formation between PVIm and PMAA

H. T. van de Grampel,† Y. Y. Tan,* and G. Challa

Laboratory of Polymer Chemistry, State University of Groningen, Nijenborgh 16, 9747 AG Groningen, The Netherlands

Received March 27, 1991; Revised Manuscript Received October 8, 1991

ABSTRACT: The significance of kinetic processes influencing complex formation in template polymerization of *N*-vinylimidazole along poly(methacrylic acid) (PMAA) in water has been demonstrated by relating the pH at incipient complexation to monomer conversion in the template system. In addition, calorimetric measurements showed that complexation between poly(*N*-vinylimidazole) (PVIm) and PMAA was optimal in a 1:1 base molar ratio at pH 5.95, producing the highest heat. From these, PVIm radical complexation with the template and the subsequent occurrence of template effects could be rationalized. Polymerization rate enhancements at different reaction conditions were not related to aggregation processes. On examination of DSC traces and FTIR spectra, it is found that anhydride formation at elevated temperatures is partially suppressed in template-formed complexes. It is proposed that template-formed complexes possess an enhanced degree of interaction as compared to synthetic complexes. Prolonged growth along templates of greater length leads to template complexes with a composition of PMAA to PVIm approaching 1:1 in monomeric units.

1. Introduction

The process in which radicals propagate alongside template macromolecules is referred to as template radical polymerization.[1] The significance of complexation in template polymerization is obvious since complexation of a growing radical with the template is required before template growth is possible. This complexation process involves cooperative interactions between the template and growing radical, and the complexation constant therefore determines the number of template-associated radicals which effectuates the template effect.[2-4] In addition, it is generally accepted that the in situ complex formation by template polymerization leads to ladder-type complexes in which a more efficient complexation can be achieved than by mixing of the two ready-made polymers.[1,2]

One of the intriguing features of template polymerization is the thermodynamically driven process of complexation in a kinetic process like polymerization. Consider the usual approach of increasing the template concentration at constant monomer concentration to determine the polymerization mechanism. In the kinetic or diffusion framework, this procedure enhances the probability that a radical of any length may find a template chain to complex with before it terminates. For a thermodynamically determined process, it has been established that the critical chain length for complexation is inversely dependent on the template concentration.[5,6] If complexation and subsequent radical propagation along the template is found to occur only beyond a certain minimal template concentration, it does not point to only one of the theories.

Template polymerization generally leads to rate enhancements with respect to conventional polymerizations, expressed in relative rate, R_{rel}. We already reported on the template effects in the template polymerization of *N*-vinylimidazole (VIm) along poly(methacrylic acid) (PMAA), using 2,2′-azobis(2-amidinopropane)·2HCl (AAP) as initiator.[7-9] Three regions could be distinguished in the plot of R_{rel} versus [PMAA] at constant $[VIm]_0$, viz., region A at $[PMAA]/[VIm]_0 < 0.45$ with $R_{rel} = 1$, i.e., no rate enhancement, region B for $0.45 < [PMAA]/[VIm]_0 < 1$ with R_{rel} increasing, and region C for $[PMAA]/[VIm]_0 > 1$ with a nearly constant but elevated R_{rel}.[7] The AB transition which coincided with incipient complex formation was explained by beginning template propagation of radicals which have achieved the critical chain length necessary to complex with the template. The BC transition was attributed to the complexation and subsequent propagation of the maximum amount of radicals with the template.[7,8]

In the present system, the critical chain length of the radical is determined by the charge density and length of the radical, which can be influenced by pH and initiator concentration, respectively.[7] Interestingly, the critical chain length is not affected by the template concentration as predicted for a thermodynamically driven process[5,6] but by the template to monomer ratio.[8] This effect can be attributed to the presence of charges in the template system.

In this paper we intend to further substantiate the relation between radical complexation and template effect. With respect to poly(*N*-vinylimidazole) (PVIm) and PMAA, only the latter has been used in numerous complexation studies.[10,11] It may be anticipated that PVIm, being a weak polybase, behaves similar to related polybases like poly(2-vinylpyridine).

2. Experimental Section

2.1. Materials. The syntheses of PMAA[7] and PVIm[8,11] have been reported previously. Their viscosity-average molecular weights, $\bar{M}_v$, were 95×10^3 (PMAA-8), 13×10^3 (PVIm-1), 70×10^3 (PVIm-2), and 200×10^3 (PVIm-3). The synthesis of it-PMAA-4 is described in ref 7. The tacticity as determined by ^{1}H NMR and ^{13}C NMR was (mm):(mr):(rr) = 95:5:0 for it-PMAA-4 and 5:35:60 for cv-PMAA-8.

The formation of complexes by template polymerization as well as conversion measurements has been described in previous papers.[7-9] Completion of the aggregation process was determined by the visual observation of lump formation accompanied by clarification of the solution. After polymerization, complexes were separated from the supernatant solution, dried, powdered, and dried again at 45 °C in vacuum.

† Present address: General Electric Plastics, P.O. 117, 4600 AC Bergen op Zoom, The Netherlands.

0024-9297/92/2225-1041$03.00/0 © 1992 American Chemical Society

Table I
Composition of Complexes of PMAA and PVIm

code	PMAA/PVIm, mol/mol	particulars[a]
A	1.03	template complex, $[PMAA]/[VIm]_0 = 1$[b]
B	0.91	template complex, $[PMAA]/[VIm]_0 = 0.3$[b]
C	0.87	synthetic complex, $\bar{M}_{v,PVIm} = 70 \times 10^3$
D	0.87	synthetic complex, $\bar{M}_{v,PVIm} = 13 \times 10^3$
E	0.98	synthetic complex, pH 5.9, $\bar{M}_{v,PVIm} = 200 \times 10^3$
F	1.08	mixture, $\bar{M}_{v,PVIm} = 70 \times 10^3$

[a] $\bar{M}_{v,PMAA} = 95 \times 10^3$. [b] $[VIm]_0 = 0.41$ M; $[AAP]_0 = 0.047$ M.

Synthetic complexes were obtained by simultaneous mixing of the two polymers in aqueous solutions. The dispersions were stirred for 15 min and the insoluble complexes removed by filtration and dried. Compositions of template and synthetic complexes, determined by elemental analysis, are listed in Table I.

2.2. Techniques. Calorimetry. Calorimetric experiments of complexations were carried out in a Setaram Calvet Type C80 twin microcalorimeter at 50 °C. Corrections to enthalpies of dilution appeared to be unnecessary. The precision of the equipment at the conditions employed was ±5%. Each measurement was performed at least three times. Unless otherwise stated, the total polymer concentration was 4.00×10^{-3} baseM, corresponding to 0.360 g/L. Solutions were adjusted to the various pH's using 0.1 N HCl or 0.1 N NaOH solutions.

Differential Scanning Calorimetry. DSC runs were performed using a Perkin-Elmer DSC-7. A scan speed of 10 °C/min was employed in the case of the determination of the water content (first run) and anhydride formation (second run); the T_g's were determined using a scan speed of 20 °C/min (third run). Measurements were performed in duplicate.

Complexations. Complexations were performed by continuous or dropwise addition of 1.0 N HCl solution to a solution of PVIm and PMAA at 50 °C under a nitrogen atmosphere, using a digital meter equipped with an Ingold combined electrode. One set of complexations was performed starting at pH 10 and the other in the presence of *N*-vinylimidazole and NH_4Cl starting at pH 8. Incipient complexation coincided with the formation of a hazy blue precipitate. The concentration of the system had no appreciable influence on the pH at which complexation occurred, which is in line with pH measurements of the initial conditions of template polymerization.[8] The only difference appeared to be that the formed flocculent precipitates dissolved more slowly than at lower concentration, which hampered the pH measurements.

FTIR. Measurements were performed of powdered compounds in KBr pellets at ambient temperature using a Bruker IFS 88 FTIR spectrophotometer.

Wide-Angle X-ray Scattering. The powdered samples were analyzed with a Statton photograph X-ray camera using Ni-filtered Cu Kα radiation.

Complex Composition. Complex composition was determined using elemental analysis and ^1H NMR (Varian 300 MHz) of solutions in D_2O at pD 1.

Micrographs. A Zeiss polarization microscope was used equipped with a camera.

3. Results and Discussion

3.1. Complex Formation and Aggregation. Generally, three stages may be discerned in the complexation of two polymers: complexation at the level of monomeric units leading to complexed chain segments, association of complexed chain segments resulting in compact particles and aggregation of these particles, eventually followed by flocculation. In the case of a polyelectrolyte complex, redistribution of interactions within the complex is possible to obtain a more stable complex[10,12] in which respect it differs from complexation between two nonionic polymers. Intercomplex association and aggregation take place mainly through hydrophobic interactions.

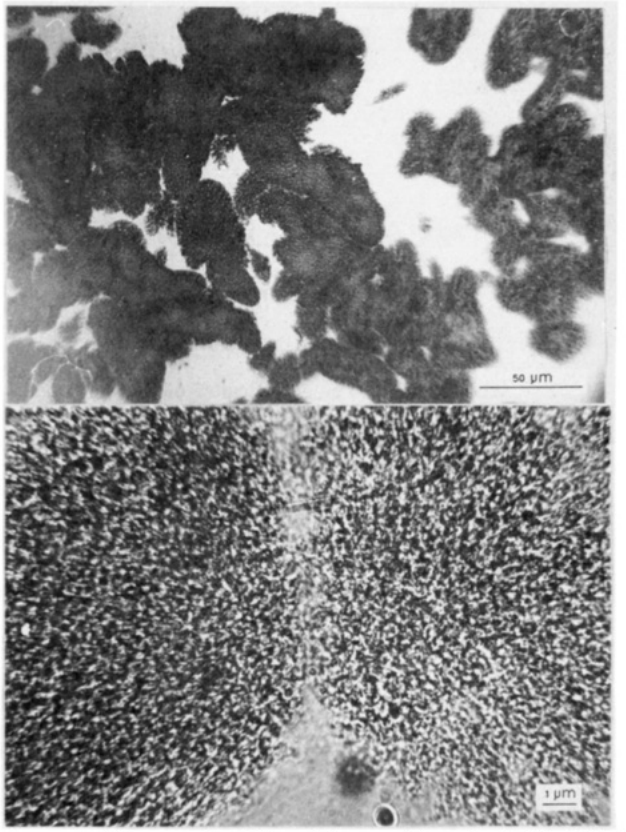

Figure 1. Micrographs of template complexes in which radical growth continues. Conditions: $[PMAA]/[VIm]_0 = 1$, 15% monomer conversion.

The same three stages are visible in template polymerization, although in this particular case the complexes are formed by polymerization instead of mixing ready-made polymers. At the initial stage of the reaction the mixture becomes hazy blue owing to radical complexation with the template. In time and with increasing monomer conversion, this turns into a milky white dispersion of small particles which gradually become coarser and eventually aggregate to a white lump within a clear reaction mixture. It should be stressed that conversion versus time curves[7] show no break after this, signifying that template polymerization is still possible within the aggregated precipitate. However, it is conceivable that complexation of new radicals is no longer feasible beyond this point. Additionally, one may expect that the aggregation process is affected by the effectiveness and rate with which the hydrophobic complexed chain parts are formed by the template polymerization. Using this link between radical propagation and aggregation, we attempted to quantify the aggregation process.

In Figure 1, a micrograph of the milky white dispersion shows both the small dimension in the order of 200 μm and the large number of the particles within which template polymerization takes place. These particles gradually aggregate to larger ones until a big lump is formed with clarification of the reaction mixture. This marks the completion of the aggregation process characterized by t_{ag} and α_{ag}, being the time and monomer conversion at this point, respectively. Obviously, t_{ag} is related to the rate of aggregation, but it is unclear how the variables are linked to the polymerization process and the template propagation in particular.

The variables are dependent on the polymerization conditions. They are shifted to higher values on increasing the template concentration at a constant $[VIm]_0$ of 0.41

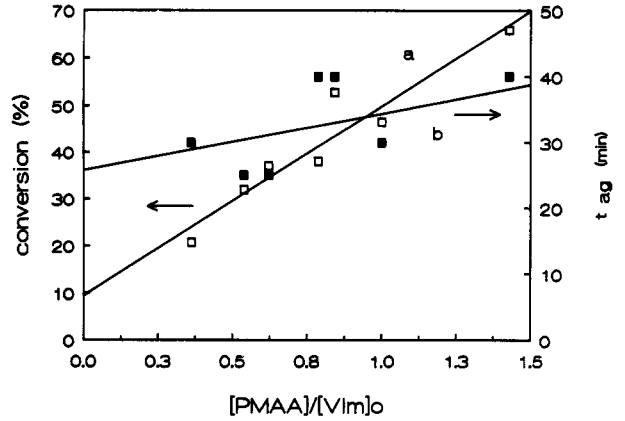

Figure 2. Influence of $[PMAA]/[VIm]_0$ at a constant $[VIm]_0$ of 0.41 M on monomer conversion α_{ag} (curve a, □) and time t_{ag} (curve b, ■) at completion of the aggregation process. $[AAP]_0$ = 0.047 M.

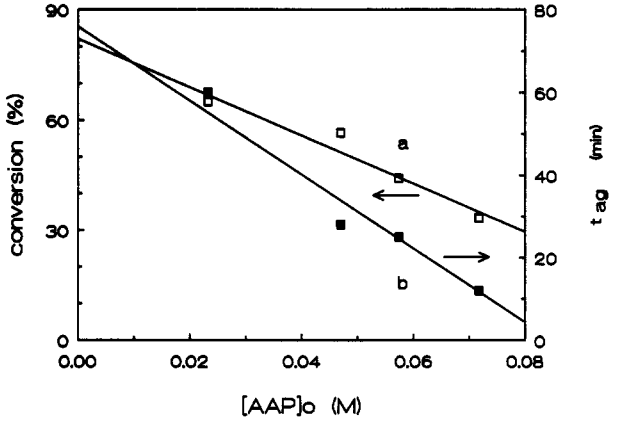

Figure 3. Influence of $[AAP]_0$ on monomer conversion α_{ag} (curve a, □) and time t_{ag} (curve b, ■) at completion of the aggregation process. $[PMAA]/[VIm]_0$ = 1.0; $[VIm]_0$ = 0.41 M.

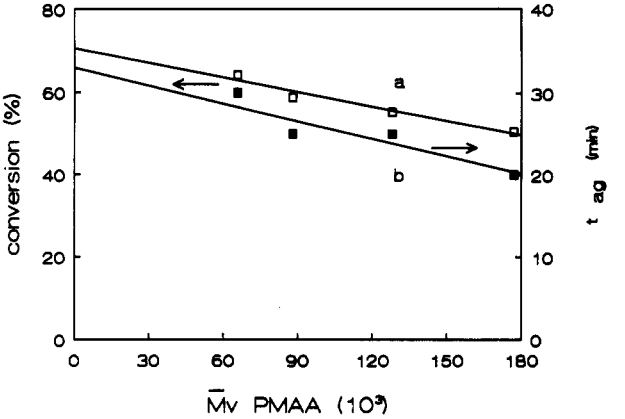

Figure 4. Influence of template molecular weight on monomer conversion α_{ag} (curve a, □) and time t_{ag} (curve b, ■) at completion of the aggregation process. $[PMAA]/[VIm]_0$ = 1.0; $[VIm]_0$ = 0.41 M; $[AAP]_0$ = 0.047 M.

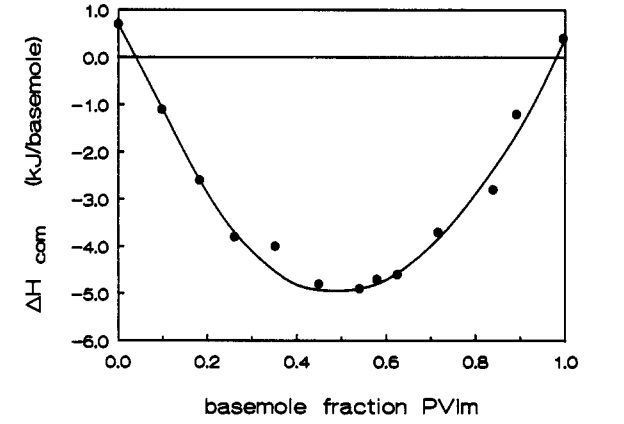

Figure 5. Heat of complexation (ΔH_{com}) of PVIm with PMAA in aqueous solution versus basemolar fraction of PVIm at 20 °C. $\bar{M}_{v,PVIm}$ = 70 × 10³; $\bar{M}_{v,PMAA}$ 95 × 10³.

M (Figure 2). Especially α_{ag} demonstrates a strong increase, which can be linked to the trend in rate enhancements. It is known that higher rate enhancements are obtained at higher $[PMAA]/[VIm]_0$ due to more radicals growing alongside the template as well as a longer radical propagation alongside the template. Both these factors contribute to a higher monomer conversion at which the template process, and thus the complexation, is accomplished. Consequently, α_{ag} seems related to the efficiency of complexation.

Also, both t_{ag} and α_{ag} depend on the initiator concentration (Figure 3). Increasing [AAP] leads to a faster aggregation process (shorter t_{ag}) which is undoubtedly caused by the higher rate of polymerization. Interestingly, t_{ag} and α_{ag} run parallel to rate enhancement (R_{rel}) defined as the ratio of $R_p([PMAA]/[VIm]_0 = 1.0)$ to $R_p([PMAA]/[VIm]_0 = 0.2)$, which increases from 4 at $[AAP]_0$ = 0.072 M to 8 at $[AAP]_0$ = 0.024 M.[8] Again, α_{ag} seems related to the template effect, i.e., the efficiency of radical growth alongside the template chain.

By contrast, shorter t_{ag} and lower α_{ag} are obtained on increasing the template molecular weight (Figure 4), whereas accompanying rate enhancements increase from 4 using $\bar{M}_{v,PMAA} = 30 \times 10^3$ to 7.2 for $\bar{M}_{v,PMAA} = 177 \times 10^3$ due to a longer radical growth period along the same template chain.[8] To reconcile this behavior with the previously mentioned interpretation of α_{ag} and t_{ag}, we have to take account of the fact that growth of a radical is not restricted to only one template chain since radicals are able to hop between templates.[9] Furthermore, lower monomer conversions are sufficient for a radical to form a complex with two long chains than many short template chains with the same total length. The aggregation process in the case of longer template chains is thus completed at lower α_{ag} values. This phenomenon also demonstrates that one cannot follow the template polymerization process by simply measuring α_{ag}.

3.2. Complexation during Polymerization. In Figure 5, it can be seen that complexation between PVIm and PMAA takes place in a 1:1 basemole ratio which reflects the interaction of one COOH group with one imidazole ring. This is not self-evident considering the fact that complexation between PVIm and PMAA is strongly dependent upon the amount of reactive groups[7,8,11] which is determined by pH.

Complexation of radicals with the template is required before template polymerization can take place. In template polymerization these complexes are formed in situ. Usually the system contains more template molecules than PVIm radicals formed, though this actually depends on the initial template to monomer ratio, $[AAP]_0$, and conversion. In addition the system comprises adsorbed and free monomer molecules as well as ions derived from the initiator (cations and Cl^- ions). All these factors may have a substantial effect on the complexation behavior of the two polymers.

We will now try to determine how this radical complexation is influenced by the presence of monomer and initiator, as well as the continuously changing complexation conditions, i.e., pH, [VIm], available PMAA and

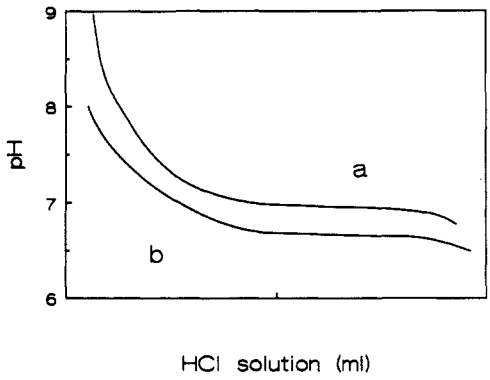

Figure 6. Potentiometric titration curve of PMAA–PVIm solution (curve a) and PMAA–PVIm–VIm (10:1:9) solution (curve b). Temperature 50 °C $\bar{M}_{v,PVIm} = 13 \times 10^3$, $\bar{M}_{v,PMAA} = 95 \times 10^3$.

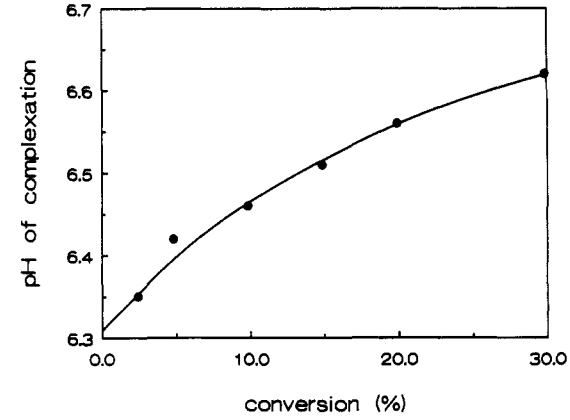

Figure 7. Influence of monomer conversion, as simulated by the PVIm/VIm ratio, on the pH of complexation at 50 °C.

PVIm, etc. First, to illustrate the impact of monomer and initiator, the following complexation experiments were performed. (All concentrations are denoted in units of mol dm^{-3} (≡baseM).) A mixture of PVIm and PMAA with [PMAA]/[PVIm] = 1 was dissolved at pH 11 and subsequently titrated with HCl solution (Figure 6, curve a). The pH of the solution shows a gradual decrease down to pH 7 after which the curve deflects and the solution becomes turbid due to complexation between PVIm and PMAA. A similar experiment was done in which polymerization conditions were simulated at $[PMAA]/[VIm]_0 = 1$ and 10% monomer conversion leading to [PMAA]/[PVIm] = 10 and [VIm] = 0.36 M (Figure 6, curve b). The effect of the initiator AAP was simulated by adding NH_4Cl[9] to a concentration which nearly coincided with that of Na^+ and Cl^- present in the first-mentioned experiment whereby the pH was reduced from 11 to 7. The lower pH of 6.7 on complex formation is probably related to the presence of adsorbed VIm which affects the accessibility of template sites for complexation.

AB Transition. Second, we focus on the continuously changing complexation conditions, using the AB transition as a test case. We have already established[8] that the pH is regulated by the $[PMAA]/[VIm]_0$ ratio and determines whether or not a radical possesses a charge density sufficient to associate with the template chain which is subsequently followed by template polymerization. These critical conditions coincided with the AB transition, i.e., at $[PMAA]/[VIm]_0 = 0.45$ for $[AAP]_0 = 0.047$ M.[7,8] Furthermore, incipient complexation in template polymerization takes place mainly by electrostatic interactions instead of hydrogen bonds.[7] This is corroborated by experiments by Tsuchida et al.,[13] who showed that complexation between PMAA and a hydrogen-bond-accepting polymer like poly(ethylene oxide) is not feasible at pH 6, whereas it is possible between PMAA and poly(2-vinylpyridine) where electrostatic interactions play a role.

The pH at the AB transition is 6.39, which is lower than the obtained value of 6.7 and 7.0 for the complexation experiments mentioned above. Initial complexation of a radical with the template in a template polymerization should thus be feasible at a lower template to monomer ratio than the obtained ratio of 0.45.[7]

To demonstrate the kinetic aspects of complexation in template polymerization near the AB transition, template polymerization conditions were simulated by performing complexations with ready-made polymers using different ratios of PVIm to PMAA while maintaining a constant concentration of monomeric VIm units, i.e., [PVIm] + [VIm] = constant. The ratio [PMAA]/([PVIm] + [VIm]) = 0.4 was chosen to ascertain why complexation does not occur at this ratio prior to the AB transition. To simulate the template system even better, NH_4Cl was added to compensate for the absence of the initiator AAP and a low molecular weight PVIm ($\bar{M}_v = 13 \times 10^3$) corresponding to the average radical length[7] was used (see ref 9 for the effect of NH_4Cl on the template polymerization). In order to relate the results to template polymerization, [PVIm] to [VIm] ratios were converted to monomer conversion (Figure 7).

Incipient complex formation was taken as the point where the solution turned hazy blue by the addition of HCl solution. From Figure 7, where the pH of incipient complexation is plotted versus the calculated monomer conversion, it is seen that complexation takes place at a higher pH with increasing monomer conversion. Translated to the template polymerization system, complexation is less feasible at a low monomer conversion and PVIm radicals require a higher charge density, i.e., lower pH, to achieve complexation. This may be explained by the mentioned presence of adsorbed VIm rendering PMAA sites inaccessible for complexation. In terms of template polymerization this means that complexation and template growth become more feasible with increasing conversion. This effect is enhanced considering the fact that the pH of the template system is reduced by 0.2 pH units during the polymerization up to 100% conversion. From the plot of pH versus the initial conditions,[7] one obtains a pH of 6.41 at $[PMAA]/[VIm]_0 = 0.4$. Consequently, judging from Figure 7, complexation and rate enhancement in the template polymerization should become feasible at 5% monomer conversion. This was not observed, however, although tacky transparent complexes were obtained. Obviously, PVIm which is formed in the initial stage does have interactions with PMAA, but the associate remains in solution.

Two explanations may be forwarded for the absence of rate enhancements beyond 5% monomer conversion. First, since PMAA is relatively strongly charged, it can interact with many short PVIm chains which are barely protonated.[7] We propose that this associate formation leads to a removal of template chains from the reaction mixture such that none is available by the time 5% monomer conversion is achieved. Second, it is possible that template growth takes place but does not lead to higher rates under these conditions.

Rate enhancements are obtained if the $[PMAA]/[VIm]_0$ in the template polymerization is increased beyond the AB transition. The addition of more template to the system leads to a reduction of the initial pH, which enables complexation to occur at a lower monomer conversion. Furthermore, it will be more difficult for the PVIm formed

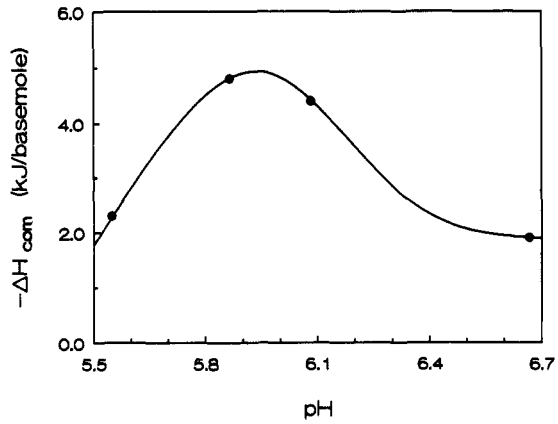

Figure 8. Influence of $pH^{50°C}$ on heat of complexation (ΔH_{com}) using [PMAA]/[PVIm] = 1. $\bar{M}_{v,PVIm} = 13 \times 10^3$; $\bar{M}_{v,PMAA} = 95 \times 10^3$.

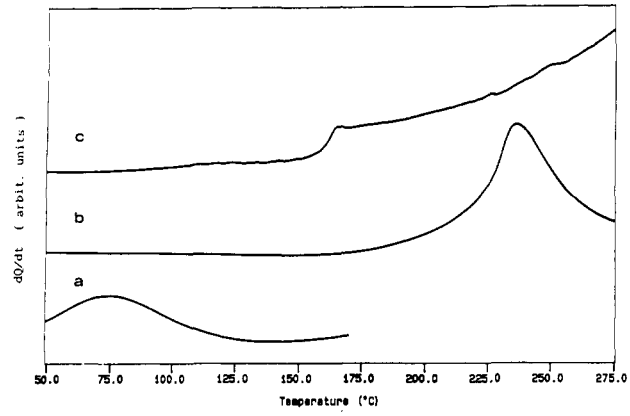

Figure 9. Typical DSC curves. First run: water removal (curve a). Second run: anhydride formation (curve b). Third run: T_g determination of the formed an-PMAA (curve c). Scan speeds are 10 °C/min for the first two runs and 20 °C/min for the third run.

to remove all the template chains by complexation from solution in the early stages of the polymerization. Hence, from the above we can state that in addition to a thermodynamic process, i.e., the existence of a critical chain length,[7] also a kinetic process is affecting complexation in this template polymerization. Moreover, since the pH and monomer conversion are the two determining factors, this statement also holds for different $[VIm]_0$ and $[AAP]_0$ for which related AB and BC transitions were obtained.[8]

BC Transition. Knowing that changing polymerization conditions can have an impact on the complexation behavior, we now focus on the BC transition which has been attributed to maximum radical complexation[7] and which differs by only a 0.5 pH unit with the AB transition, the onset of incipient complexation. The degree of complexation, expressed in terms of complexation heat, is shown in Figure 8 as a function of pH. It is apparent that complexation between PVIm and PMAA at the particular ratio of [PMAA]/[PVIm] = 1 is at its best at pH 5.95, which coincides with the pH of polymerization reaction mixtures at $t = 0$ min and $[PMAA]/[VIm]_0 = 1.1$.[7]

Furthermore, it is important to note that the heat of complexation varies by a factor of 2 over a narrow pH range. Though the calorimetric experiment measures the overall complexation process, the time scale of the complexation process cannot be completely ignored as was discussed in the previous paragraph. Nevertheless, the assumption that a maximum complexation of radicals is achieved at the BC transition seems hereby to be justified.

The decreasing complexation at lower pH's would imply that rate enhancements should reduce in region C, i.e., beyond the BC transition. However, since the maximum heat of complexation is determined by an optimal ratio of anionic and cationic sites, we may expect a maximum complexation at lower pH if higher ratios of PMAA to PVIm are used. Consequently, the nearly constant rate enhancement beyond the BC transition may still involve a maximum amount of template-associated radicals, especially in view of the high template concentration.

3.3. Complex Characterization. In this section, we intend to demonstrate that template polymerization leads to complexes in which complexation is accomplished to a higher degree as compared to synthetic complexes. It seems reasonable to expect that template polymerization leads to better ordered complexes of the ladder type due to the in situ formation of the second polymer component. However, WAXS patterns of a template complex, a synthetic complex, and the two constituent polymers exhibited only broad bands.

The following complexes, listed in Table I, were studied: template complexes prepared at $[PMAA]/[VIm]_0$ ratios of 0.3 (A) and 1.0 (B), and synthetic complexes prepared with PVIm having a $\bar{M}_v$ of 70×10^3 (C) and 13×10^3 (D). The last molecular weight corresponds approximately to the length of the oligomeric PVIm radicals in template polymerizations.[7] Furthermore, a complex E was obtained by mixing PVIm-3 ($\bar{M}_v = 200 \times 10^3$) with PMAA-8 at pH 5.9.

Thermal Properties. DSC provides another means to distinguish differences between template complexes and synthetic complexes. The main characteristics of the DSC traces in relation to the preparative method of the samples will be discussed.

Typical DSC traces are shown in Figure 9. In the first run from 30 to 160 °C (curve a), the endothermic peak near 75 °C is due to removal of water from the sample which in all cases corresponds to a weight loss of approximately 5%. In the second run from 30 to 280 °C (curve b), the endothermic peak near 235 °C seems to be caused by the anhydride formation for which a temperature of 200 °C has been reported.[14-16] In a third run at a scan speed of 20 °C/min (curve c), the T_g of the formed anhydro PMAA (an-PMAA) is revealed. The weight loss after the second run can thus be attributed to anhydride formation. However, theoretically, only 87% of the maximum amount of intramolecular anhydride groups can be formed, the deviation from 100% being caused by the inaccessibility of isolated COOH groups.[17,18] This corresponds to a 9% weight loss of the PMAA sample, which is substantially lower than those found (Table II). It is also apparent from Table II that the deviation from the theoretical weight loss is not related to PVIm which binds water strongly at the imidazole ring.[19,20] Consequently, degradation of PMAA must have taken place to some extent.[16]

The excess loss of weight may also be explained by liberation of water, which has become encapsulated in the salt bonds of the complex during complex formation.

Expansions of the second run for the different complexes (Figure 10) show that the peaks do not coincide with each other, despite the identical thermal history of the samples (powders). Two tentative explanations may be forwarded for these differences in the temperature at the top of the endothermic peak (referred to as T_{max}). The first one is that T_{max} may be related to the ease with which (mainly intramolecular) anhydride formation is possible and, thus, to the spatial orientation of COOH groups (cf. T_{max} of

Table II
Some Characteristics of PMAA and PVIm and Their Complexes from DSC and FTIR Measurements

	DSC			FTIR	
sample	wt loss,[a,b] %	T_{max},[a] °C	T_g,[c] °C	$PVImH^+$,[d] %	COO^-,[e] %
A	15.6	224	194	32	8
B	31.7	216	198	35	14
C	13.7	226	193	19	2
D	12.2	230	193	25	5
E	nd	227	196	37	14
F	15.1	234	163 and 192	0	0
cv-PMAA	12	238	163		0
PVIm	0	nd	nd	0	
it-PMAA	25.4	196	150		0
$PVImH^+$	0	nd	nd	99	

[a] After second DSC run. [b] Based on PMAA content. [c] On third run. [d] Calculated from $A_{1573}/(A_{1500} + A_{1573})$. [e] Calculated according to ref 23; nd = not determined.

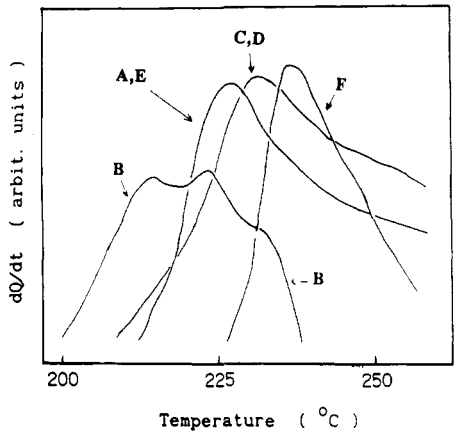

Figure 10. Expansion of the second endothermic peak for the five complexes (A–E) and PMAA–PVIm mixture (F). For samples A–F, see Table I.

isotactic PMAA and conventional PMAA in Table II). If this is the case, interactions between PVIm and PMAA in a template complex could lead to a favorable orientation of the COOH groups such that anhydride formation is facilitated. Consequently, T_{max} is lowered with respect to free cv-PMAA. Thus, complex B would possess the most favorable oriented PMAA, having the lowest T_{max}. Sample F, which is a mixture of cv-PMAA and PVIm, has approximately the same T_{max} as cv-PMAA (Table II).

The other explanation for the differences in peak location involves the stability of the complexes formed. Complex dissociation is also an endothermic process which could cause differences in peak location. An expansion of the third DSC run of complex E is shown as a broken line in Figure 11 to which a base-line correction has been applied. Although the transition seems to be a T_g, an endothermic peak is notable. This may be caused by complex dissociation or enthalpy recovery, the latter reflecting the thermal history of the sample. To discern between these two possibilities, the sample was cooled down at 200 °C/min to 30 °C and a fourth scan was performed with a scan speed of 20 °C/min (drawn line in Figure 11). The disappearance of the endothermic peak is consistent with a behavior predicted for enthalpy recovery.[21] Consequently, the presence of a T_g of the anhydro PMAA in the third run indicates that complex dissociation has occurred during the second run besides anhydride formation. The higher T_g's of 192–198 °C for the complexes on the third run as compared to the T_g of an-PMAA (163 °C) are probably caused by interactions with PVIm. No T_g of free PVIm (178 °C) was detected.

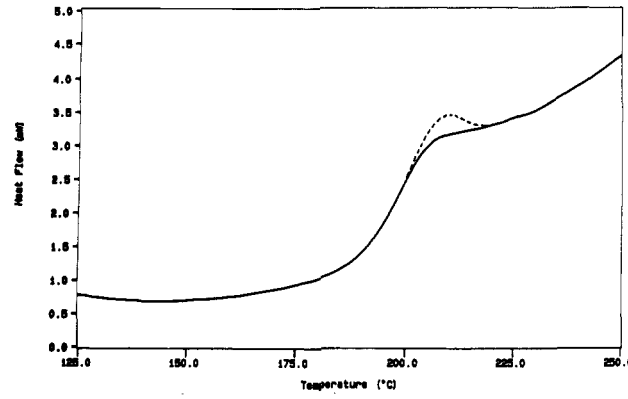

Figure 11. Third DSC run (- - -) using sample E (see Table I) and a scan speed of 20 °C/min, followed by rapid cooling of the sample at 200 °C/min and a fourth DSC run (—) employing a scan speed of 20 °C/min.

FTIR. The interactions in the complexes may be deduced from the FTIR spectra. In order to do this, we will discuss the spectra of the components first (Figure 12). The assignment of spectral bands to the various vibration modes has been reported for PVIm[19,20] and PMAA.[22,23] Though samples were dried prior to recording of the spectra, the broad feature in the 2800–3700-cm^{-1} region (Figure 12) still indicates the presence of residual bound water.[19,20]

The effect of protonation of PVIm on the FTIR spectra has been investigated by Lippert et al.[19] They were able to relate the extent of protonation to the relative absorptions of the N–H stretching vibration at 2480 and 2610 cm^{-1} (in $PVImH^+$) and the stretching and in-plane-bending vibrations of the ring at 915 cm^{-1}. In complexes, the presence of PMAA interferes with the spectrum of PVIm at these positions (Figure 12), however. Instead, we used the shift of the stretching vibration of C–C and C–N from 1500 cm^{-1} (PVIm) to 1573 and 1544 cm^{-1} ($PVImH^+$), all of which are strong absorptions. The ratio $A_{1573}/(A_{1500} + A_{1573})$ is zero for ordinary PVIm, while it is 0.99 for 100% protonated PVIm and may thus serve as a measure for the degree of protonation of PVIm. The degree of ionization of PMAA in a complex may be calculated from the ratio of the asymmetric stretching vibration of the C=O in COO^- at 1560 cm^{-1} and the C=O absorption at 1700 cm^{-1} using known extinction coefficients.[23]

These ratios were applied to the spectra of a number of complexes, presented in Figure 13. Calculated percentages of $PVImH^+$ and COO^- are listed in Table II. Nearly all values of $PVImH^+$ are higher than the degree of protonation (α_N) of 0.2 for PVIm[7] at pH 6. On the other hand, the % COO^- values in complexes A, B, and E are much lower than the α_N of 0.5 for PMAA[7] at pH 6. This would indicate that a great deal of charge neutralization has taken place by complexation of a COO^- with a protonated imidazole ring. Complexation may also be deduced from the presence of the C=O absorption at 1700 cm^{-1} which is caused by hydrogen-bonded C=O stretching vibration in PMAA.[22-24] Consequently, calculated values for % $PVImH^+$ in Table II are probably for the greater part hydrogen-bonded imidazole rings since no distinction can be made between hydrogen bonding and electrostatic interaction.[19] On the basis of the data presented in Table II, no conclusive statement can be made with respect to the complexation efficiency in template complexes compared to synthetic complexes. In addition, though it is known that insoluble nonstoichiometric complexes result when more than 50% of the complementary groups has reacted,[11] this cannot be deduced from the spectra.

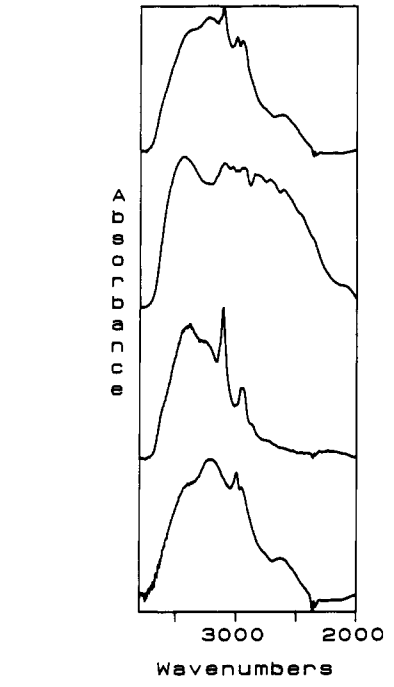

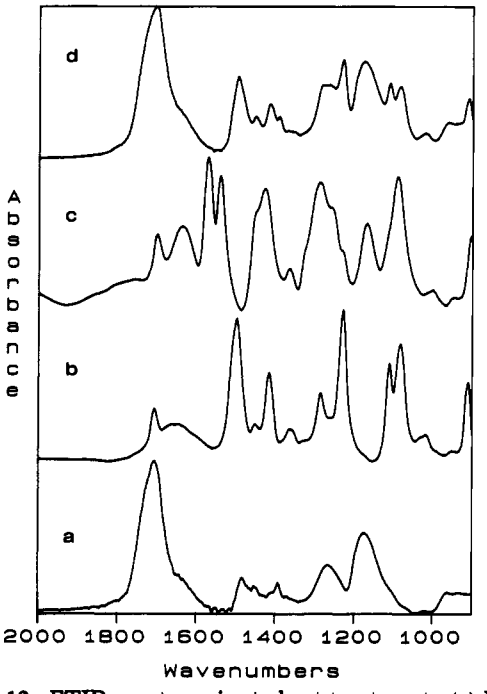

Figure 12. FTIR spectra prior to heat treatment: (a) PMAA, (b) PVIm, (c) $PVImH^+$, (d) a mixture of PMAA and PVIm (sample F).

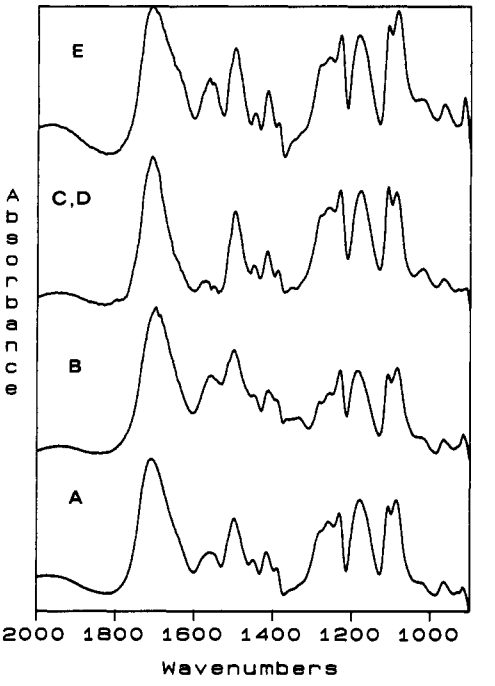

Figure 13. FTIR spectra prior to heat treatment of complexes A–E (see Table I for particulars).

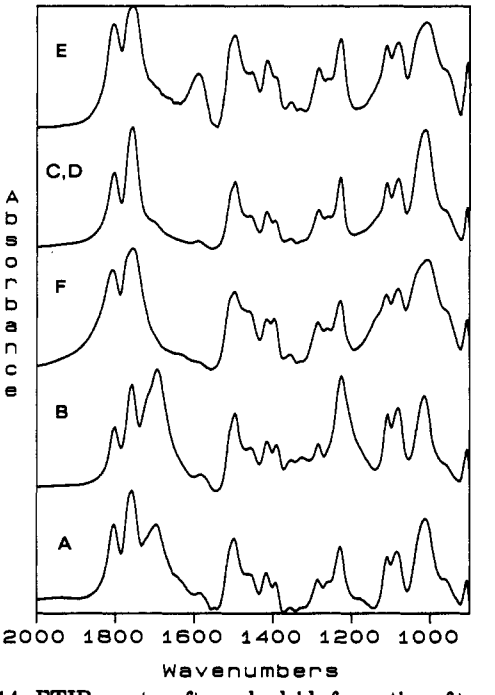

Figure 14. FTIR spectra after anhydride formation of template-formed complexes (samples A and B), synthetic complexes (samples C–E), and a mixture of PMAA and PVIm (sample F).

In Figure 14 FTIR spectra of complexes after the second DSC run (anhydride formation) are shown covering the region 900–2000 cm^{-1}. Anhydride formation is obvious from the C–O–C band at 1020 cm^{-1} and the two bands at 1758 and 1801 cm^{-1} which have been ascribed to the asymmetric and symmetric stretching vibrations of C=O, respectively.[16,18,24] In addition, PMAA is still present as may be deduced from the broad band at 1700 cm^{-1}.[22-24] The absorption at 1580 cm^{-1} in the case of complex E is presumably caused by the asymmetric stretching vibration of the C=O in COO^-.[23] Interestingly, the ratio between the anhydride absorptions and PMAA absorptions differs for the various complexes (cf. complex A with complexes C and E). The template-formed complexes still have a large absorbance caused by the hydrogen-bonded COO, and apparently not all COO groups have been converted to anhydride rings. Anhydride formation is thus suppressed in the case of template-formed complexes.

This different behavior of the template versus synthetic complexes with respect to the anhydride formation of PMAA may be explained by summarizing DSC and FTIR results: (1) anhydride formation in template complexes is facilitated indicating orientation of COO groups, (2) a T_g of an-PMAA is visible pointing to complex dissociation, and (3) anhydride formation is partially suppressed in the case of template complexes. Facilitation of anhydride formation can only be reconciled with a reduced anhydride formation if we assume that part of the PMAA chain is not capable of forming anhydride rings because it is too well complexed in a ladder-type structure. We propose

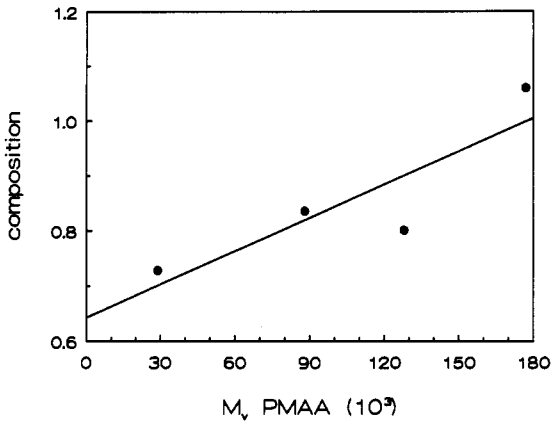

Figure 15. Basemolar composition of the template complex versus template molecular weight. Conditions: $[PMAA]/[VIm]_0 = 1.0$, $[VIm]_0 = 0.41$ M, $[AAP]_0 = 0.047$ M, and the monomer conversion is 95%.

that these well-complexed chain sections result from radical propagation alongside the template chain. A template complex would then consist of short well-complexed chain sections alternated with longer sections possessing randomly complexed and noncomplexed COOH groups. Only those chain sections intermediate of the well-complexed parts will form anhydride rings and eventually give rise to a T_g.

3.4. Composition of the Template Complex. From a comparison between polymerization conditions and complex composition, it is possible to obtain information concerning the amount and effectiveness of radical propagation alongside the template. By using a weak polyacid or polybase in combination with a strong complementary polyelectrolyte, the dissociation state of the weaker polyelectrolyte directly determines the composition of the obtained complex. In the present system, both PMAA and PVIm are weak polyelectrolytes. However, it is known that complexation may induce enhanced dissociation behavior of the constituent polymers,[10,13,25,26] which is caused by the reduction of intramolecular electrostatic repulsions between the charged groups. Complex composition is therefore more difficult to predict. Template complexes were not compared with synthetic complexes, since almost all preparation methods of the latter lead to a 1:1 stoichiometry.[10,11]

In Figure 15, it is shown that the composition of template complexes becomes unity with increasing template molecular weight. In addition rate enhancements increase from 4 using $\bar{M}_{v,PMAA} = 30 \times 10^3$ to 7.2 for $\bar{M}_{v,PMAA} = 177 \times 10^3$ due to a longer radical growth period along the same template chain.[8] First, it seems evident that template growth should theoretically lead to PMAA/PVIm = 1 due to radical growth along the entire template chain, but account should be taken of the incomplete usage of the template by the radical. Statistically, the oligomeric radical will use only half of the template length since it may complex at any position on a template macromolecule and propagate in either direction. Consequently, this leads to a PMAA to PVIm ratio of 2 in the initial stage of the polymerization. The remaining parts of the template may be used by other radicals, thereby reducing PMAA/PVIm to 1.

The other way of reasoning is focused on the degree of neutralization, α_N, of both polymers. In this respect we shall ignore the reduction of pH during the template polymerization whereby monomer is converted to the less basic polymer. Polymerization conditions at $[PMAA]/[VIm]_0 = 1$ and $[VIm]_0 = 0.41$ M lead to $\alpha_{N,PMAA} = 0.48$ and $\alpha_{N,PVIm} = 0.19$.[7] Thus, charge neutralization will lead to a complex composition of PMAA/PVIm = 0.4. The complex composition approaching 1 with increasing template molecular weight (Figure 14) indicates that both explanations are valid.

4. Conclusions

The importance of complexation in template polymerization has been demonstrated by using a variety of techniques. A link was established between complexation studies and radical complexation in template polymerization.

The resulting complexes are different from synthetically made complexes. This is ascribed to a higher and different degree of interaction in the template complexes. More experiments are necessary, however, to determine the exact complex structure resulting from radical growth along the template.

Acknowledgment. This study was supported by The Netherlands Foundation for Chemical Research (SON) with financial aid from The Netherlands Organization for Scientific Research (NWO). We thank Mr. G. O. R. Alberda van Ekenstein for assistance with the DSC experiments.

References and Notes

(1) Tan, Y. Y.; Challa, G. *Encyclopedia of Polymer Science and Engineering*; Mark, H. F., Bikales, N. M., Overberger, C. G., Menges, G., Eds.; Wiley: New York, 1989; Vol. 16, p 554.
(2) Smid, J.; Tan, Y. Y.; Challa, G. *Polym. Commun.* **1986**, *27*, 148.
(3) Koetsier, D. W.; Tan, Y. Y.; Challa, G. *Polymer* **1981**, *22*, 1709.
(4) Bartels, T.; Tan, Y. Y., Challa, G. *J. Polym. Sci., Polym. Chem. Ed.* **1977**, *15*, 341.
(5) ten Brinke, G.; Schomaker, E.; Challa, G. *Macromolecules* **1985**, *18*, 1925.
(6) Schomaker, E.; ten Brinke, G.; Challa, G. *Macromolecules* **1985**, *18*, 1930.
(7) van de Grampel, H. T.; Tan, Y. Y.; Challa, G. *Macromolecules* **1990**, *23*, 5209.
(8) van de Grampel, H. T.; Tan, Y. Y.; Challa, G. *Macromolecules* **1991**, *24*, 3767.
(9) van de Grampel, H. T.; Tan, Y. Y.; Challa, G. *Macromolecules* **1991**, *24*, 3773.
(10) Tsuchida, E.; Abe, K. *Adv. Polym. Sci.* **1982**, *45*, 1.
(11) Phillip, B.; Dautzenberg, H.; Linow, K.-J.; Kötz, J.; Dawydoff, W. *Prog. Polym. Sci.* **1989**, *14*, 91.
(12) Kabanov, V. A.; Zezin, A. B.; Rogacheva, V. B.; Grishina, N.; Goethals, E.; Van de Velde, *Makromol. Chem.* **1986**, *187*, 1151 and references therein.
(13) Abe, K.; Koide, M.; Tsuchida, E. *Macromolecules* **1977**, *10*, 1259.
(14) Lohmeyer, J. H. G. M. Ph.D. Thesis, State University of Groningen, Groningen, The Netherlands, 1979 (in Dutch).
(15) Lohmeyer, J. H. G. M.; Kransen, G.; Tan, Y. Y.; Challa, G. *J. Polym. Sci., Polym. Lett.* **1975**, *13*, 725.
(16) Grant, D. H.; Grassie, N. *Polymer* **1960**, *1*, 125.
(17) Flory, P. J. *J. Am. Chem. Soc.* **1939**, *61*, 1518.
(18) Semen, J.; Lando, J. B. *Macromolecules* **1969**, *2*, 570.
(19) Lippert, J. L.; Robertson, J. A.; Havens, J. R.; Tan, J. S. *Macromolecules* **1985**, *18*, 63.
(20) Eng, F. P.; Ishida, H. *J. Appl. Polym. Sci.* **1986**, *32*, 5021.
(21) Bosma, M.; ten Brinke, G.; Ellis, T. S. *Macromolecules* **1988**, *21*, 1465.
(22) Dechant, J. Utrarotspektroskopische Untersuchungen an Polymeren, Akademie Verlag, Berlin, 1972 (in German).
(23) Leyte, J. C.; Zuiderveld, L. H.; Vledder, H. J. *Spectrochim. Acta* **1967**, *23A*, 1397.
(24) Socrates, G. *Infrared Characteristic Group Frequencies*; John Wiley & Sons: New York, 1980.
(25) Abe, K.; Ohno, H.; Nii, A.; Tsuchida, E. *Makromol. Chem.* **1978**, *179*, 2043.
(26) Tsuchida, E.; Osada, Y.; Abe, K. *Makromol. Chem.* **1974**, *175*, 583.